Journal of Molecular Catalysis A: Chemical 424 (2016) 145–152

Contents lists available at ScienceDirect

Journal of Molecular Catalysis A: Chemical

journal homepage: www.elsevier.com/locate/molcata

# Evidence for isomerizing hydroformylation of butadiene. A combined experimental and computational study

Tapan Maji[a,b], Camina H. Mendis[a,b], Ward H. Thompson[a,b,*], Jon A. Tunge[a,b,*]

[a] Department of Chemistry, University of Kansas, Lawrence, KS 66045, United States
[b] Center for Environmentally Beneficial Catalysis, University of Kansas, Lawrence, KS 66047, United States

ARTICLE INFO

*Article history:*
Received 11 June 2016
Received in revised form 27 July 2016
Accepted 21 August 2016
Available online 28 August 2016

*Keywords:*
Hydroformylation
Carbonylation
Alkene
Isomerization
Rhodium

ABSTRACT

The (DIOP)rhodium-catalyzed hydroformylation of butadiene has been shown to give among the highest selectivities for formation of adipaldehyde, which is useful for the synthesis of nylon. Herein, isomerizing hydroformylation is shown to be a mechanism that is partially responsible for this selectivity and density functional theory studies are used to reveal the detailed pathway for the requisite alkene isomerization.


## 1. Introduction

Transition-metal-catalyzed hydroformylation of olefins is one of the most important homogeneous processes for industrial production of aldehydes [1]. Hydroformylation, also known as the "oxo process" was discovered by Otto Roelen in 1938 and subsequently became a highly efficient and widely utilized industrial process for the production of oxo chemicals globally [2]. The resulting aldehydes and aldehyde-derived compounds such as alcohols, amines, carboxylic acids, and esters are also equally valuable for the synthesis of bulk chemicals [3]. As such, hydroformylation of butadiene has been suggested as an ideal process for the production of adipaldehyde.

Adipaldehyde is a potentially valuable intermediate for producing adipic acid and hexamethylene diamine (HMDA) which are key monomers for nylon-6,6 synthesis [4,5]. Currently, nylon-6,6 synthesis relies mainly on two processes [6–12]. First, adipic acid is synthesized by the oxidation of KA oil, utilizing harsh oxidizing agents such as concentrated sulfuric and nitric acids. These strong acids produce large quantities of $N_2O$ gas as a side product, which is a significant environmental concern [6–8]. The resulting adipic acid is subsequently polymerized with hexamethylenediamine (HMDA) to form nylon-6,6. HMDA is predominantly produced by Ni-catalyzed hydrocyanation, which requires extremely careful handling of toxic HCN gas [9–12].

On the basis of the environmental concerns associated with these processes, hydroformylation has emerged as a desirable alternative for adipic acid and HMDA synthesis. Interestingly, both monomers can be synthesized from a common adipaldehyde intermediate by oxidation and reductive amination. Moreover, reduction of adipaldehyde to hexane-1,6-diol would produce a third high-valued monomer for the synthesis of polyesters (Scheme 1) [1,2,13–15]. Therefore, the efficient synthesis of adipaldehyde via hydroformylation of butadiene has significant potential to become industrially valuable. [16–23]

Several groups have reported the atom-economic synthesis of adipaldehyde via the hydroformylation of 1,3-butadiene [16–23]. However, the reactions suffer from limited selectivity to the desired adipaldehyde. For example, the Ohgomori group reported 31% selectivity of adipaldehyde with a catalyst formed from rhodium(I) and the commercially available DIOP ligand [13]. In 2011, the Hofmann group reported that selectivities of up to 50% could be achieved with rhodium(I) combined with bulky bisphosphite ligands [17]. More recently, they have utilized isomerizing hydroformylation to achieve up to 73% yield of an adipaldehyde bis-acetal derivative [24]. However, for industrial practicality the selectivity and activity of the catalysts needs further improvement.

* Corresponding authors at: Department of Chemistry, University of Kansas, Lawrence, KS 66045, United States.
*E-mail addresses:* wthompson@ku.edu (W.H. Thompson), tunge@ku.edu (J.A. Tunge).

http://dx.doi.org/10.1016/j.molcata.2016.08.021
1381-1169/

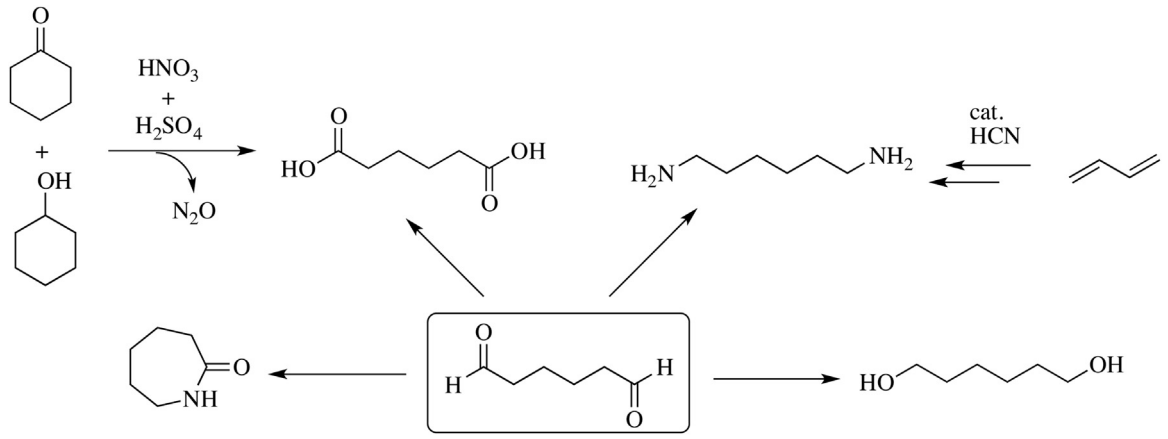


**Scheme 1.** Versatile utility of adipaldehyde.

The hydroformylation of butadiene to produce adipaldehyde requires two sequential hydroformylation reactions. Ideally, butadiene would react with syn-gas via 1,2-addition to produce pent-4-enal (Scheme 2), which is known to undergo rapid hydroformylation to form adipaldehyde [16,17]. However, the poor selectivity in hydroformylation of butadiene typically arises from the predominance of 1,4-addition in the first hydroformylation to produce pent-3-enal (Scheme 2). This product is preferentially hydroformylated to produce undesired branched aldehydes and also undergoes hydrogenation. Unfortunately, the formation of pent-3-enal is usually strongly favored both kinetically and thermodynamically. For example, dppe-ligated rhodium provides pent-3-enal with 94% selectivity [16]. Since pent-3-enal can be formed with high efficiency, we became curious whether a catalyst, or catalysts, could effect the isomerization-hydroformylation of pent-3-enal to form adipaldehyde ("our approach", Scheme 2) [25–27]. Such a process would require the development of a catalyst that is highly active for isomerization and highly selective for hydroformylation of the terminal olefin of pent-4-enal.

According to the previous report of the Ohgomori group [16], there is no indication of this type of kinetically controlled *in situ* isomerization of pent-3-enal to pent-4-enal. Hofmann, however, has recently found evidence for such a kinetic pathway with rohodium *phosphite*-catalyzed bis-hydroformylation of butadiene [24], which has been studied extensively (computationally and experimentally). Since the related reaction with the simple DIOP ligand has not been explored in detail from a mechanistic point of view, though it exhibits significant selectivity for adipaldehyde, it was of interest to study whether *phosphine*-ligated rhodium can engage in isomerizing hydroformylation.

Herein, we report the results of a combined experimental and computational study of the hydroformylation-isomerization of butadiene. It is shown that the (DIOP)Rh catalyst does indeed facilitate conversion of pent-3-enal to adipaldehyde via isomerizing hydroformylation, albeit to a limited degree. Density functional theory studies are then used to illuminate the mechanistic features of the critical olefin isomerization.

## 2. Experimental

Hydroformylation reactions were conducted using a Parr Series 5000 Multiple Reactor System. 1,3-Butadiene was obtained as a solution (20 wt.% in toluene) from Sigma-Aldrich. A typical hydroformylation of butadiene is performed in the following manner. $Rh(acac)(CO)_2$ (4.77 mg, 0.0184 mmol), DIOP (46 mg, 0.092 mmol) and 5 g of butadiene solution (20 wt.% in toluene) were added to an autoclave in the glove box. The autoclave was sealed and removed from the glove box. The autoclave was flushed by syngas ($CO/H_2$ = 1:1) at 5–6 bar pressure. The procedure was repeated three times at the same pressure to ensure the complete replacement of the Ar by syngas, and then charged by the syngas to 20 bar. The solution was stirred by 1000 rpm while being heated at 80 °C. The heating was continued for 3 h. After 3 h the autoclave was cooled to room temperature and the pressure was

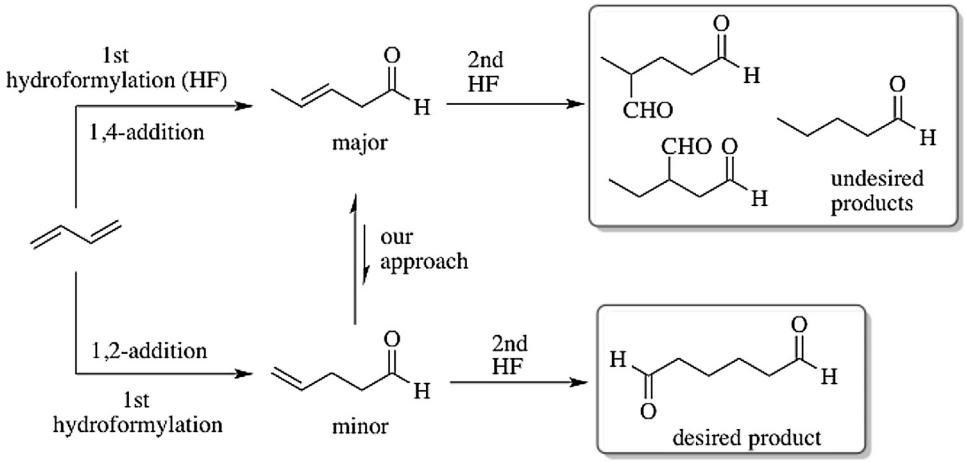


**Scheme 2.** *In situ* isomerization-hydroformylation concept.

**Table 1**
Isomerizing hydroformylation of pent-3-enal.

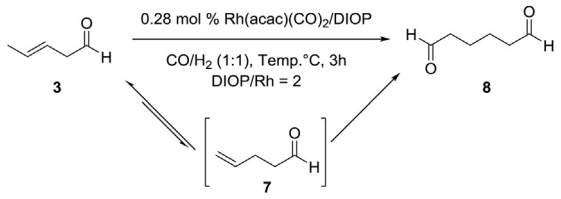


| Entry | $CO/H_2$ (bar) | Temp. (°C) | Conv. (%)[b] | %8 formed |
|---|---|---|---|---|
| 1 | 6 | 80 | 85(5) | 7.75 |
| 2 | 10 | 80 | 85(5) | 6.92 |
| 3 | 20 | 80 | 85(5) | 6.59 |
| 4 | 37 | 80 | 100 | 8.52 |
| 5 | 20 | 70 | 85(5) | 4.07 |
| 6 | 20 | 90 | 100 | 2.74 |
| 7 | 20 | 110 | 100 | 2.78 |

[a] Reaction conditions: pent-3-enal (19.5 mmol) in toluene, Rh(acac)(CO)2 (0.056 mmol), DIOP (0.11 mmol), syngas ($CO:H_2$) = 1:1.
[b] error is due to slight overlap of GC peaks for **3** and *n*-pentanal.

slowly released into a gas outlet valve inside a fumehood to avoid exposure to toxic CO. An aliquot was removed for immediate GC analysis and the product concentrations were determined from comparison to calibration curves. Pent-3-enal was produced by similar treatment of 15 g of butadiene solution (20 wt.% in toluene) with $Rh(acac)(CO)_2$ (14.33 mg, 0.056 mmol) and diphenylphosphinoethane (dppe, 22.12 mg, 0.056 mmol) for 4 h and purified by distillation at 150–160 °C. The colorless solution obtained by this way was analyzed by GC and the concentration was determined from the calibration curve. The solution can be stored under argon at low temperature (–20 °C) for 2-3 days. A 5.5 g solution of pent-3-enal in toluene (19.52 mmol) was then treated with $Rh(acac)(CO)_2$ (14.33 mg, 0.056 mmol), DIOP (55.17 mg, 0.11 mmol) at various temperatures and pressures outlined in Table 1. After 3 h, an aliquot (150 mg) was removed from the reaction mixture and added to a 10 mL volumetric flask followed by 30 mg of decane and diluted to 10 mL with toluene. The sample was then analyzed by GC and the product concentrations were calculated from comparison to calibration curves. Gas chromatographic analysis was performed on Shimadzu QP2010 SE gas chromatograph equipped with a mass selective detector (GC–MS) using helium as carrier gas. A SHRXI-5MS (30 m, 0.25 mm ID, 0.25 um df) capillary column was used. The He flow rate was kept at 0.92 mL/min. The column temperature was initially held at 60 °C for 2 min, then ramped at 10 °C/min to 200 °C and held at this temperature for 5 min. Retention times (min) of the selected products are as follows: 1,3-butadiene (1.62), *trans*-pent-2-enal (2.71), *trans*-pent-3-enal (2.52), pent-4-enal (2.43), pentanal (2.55), 2-methylpentanedial (5.87), adipaldehyde (6.95).

## 3. Results and discussion

### 3.1. Benchmarked 1,3-butadiene hydroformylation

We started our experimental findings by establishing the benchmark hydroformylation reaction of 1,3-butadiene with (DIOP)Rh catalyst as reported by Ohgomori [16]. A toluene solution of butadiene, $Rh(acac)(CO)_2$, and DIOP ligand were exposed to syn-gas ($CO/H_2$ = 1:1) in a parallel Parr reactor at elevated temperature for several hours. The optimized conditions 18.51 mmol of 1,3-butadiene in 5 mL toluene, $Rh(acac)(CO)_2$ (0.1 mol%, DIOP (0.5 mol%), 80 °C, syn-gas (20 bar), 3 h) resulted in the full consumption of 1,3-butadiene with 32% selectivity to adipaldehyde, together with some undesired side products. The major side products were pent-3-enal (**3**) and the hydrogenation product pentanal (**6**) (Scheme 3). Hydroformylation of 1,3-butadiene can, in principal, produce a number of products including the desired adipaldehyde [17], but the catalytic (DIOP)Rh system only generated few of them (viz. **3**, **4**, **6** in Scheme 3). This minimal number of byproducts adds to our belief that proper mechanistic investigation followed by rational DIOP/condition modification can increase the selectivity for adipaldehyde (**8**). Additionally, the factors providing 32% selectivity of adipaldehyde by DIOP ligand are still unclear, and a detailed mechanistic study of 1,3-butadiene hydroformylation by the (DIOP)Rh catalyst is lacking.

### 3.2. Mechanistic investigation with DIOP ligand

The commonly accepted mechanism for 1,3-butadiene hydroformylation by the (DIOP)Rh catalyst was proposed by the Ohgomori group [16], but needs further support from theoretical and experimental investigations. The observed product distribution suggests that the first hydroformylation of 1,3-butadiene takes place by the incorporation of active catalyst Rh-H via the 1,2- and 1,4-addition pathways (Scheme 3). The 1,2-addition pathway yields pent-4-enal (**7**) via intermediate **2**, which is analogous to the hydroformylation of non-conjugated/isolated terminal olefins. The subsequent n-selective hydroformylation of the resulting pent-4-enal (**7**) provides the desired adipaldehyde (**8**). Independent hydroformylation of commercially available pent-4-enal (**7**) with (DIOP)Rh catalyst by us, and (bisphosphite)Rh by others [17,18], supports the linear hydroformylation preference to adipaldehyde (Scheme 4). Alternatively, the 1,4-addition of Rh-H proceeds via a stable $\eta^3$-crotyl complex (**1**, Scheme 3) and results in pent-3-enal (**3**), which upon a second hydroformylation produces dialdehyde **4** or **5** (while both are possible, interestingly only **4** is observed). Additionally, pentanal (**6**) formation can be rationalized by direct hydrogenation of **3** or **7** or via the double bond isomerization of pent-3-enal (**3**) to the conjugated pent-2-enal followed by rapid hydrogenation by the (DIOP)Rh catalyst [28,29].

Finally, we hypothesized that pent-3-enal (**3**) could also undergo double bond isomerization to the non-conjugated pent-4-enal (**7**), which is then rapidly hydroformylated to adipaldehyde (Scheme 2). There is currently no reported evidence in the literature for this *in situ* isomerization-hydroformylation of pent-3-enal (**3**) to adipaldehyde (**8**) with phosphine-ligated rhodium catalysts. This prompted us to investigate the possibility of the isomerization-hydroformylation of pent-3-enal to adipaldehyde, which we now discuss.

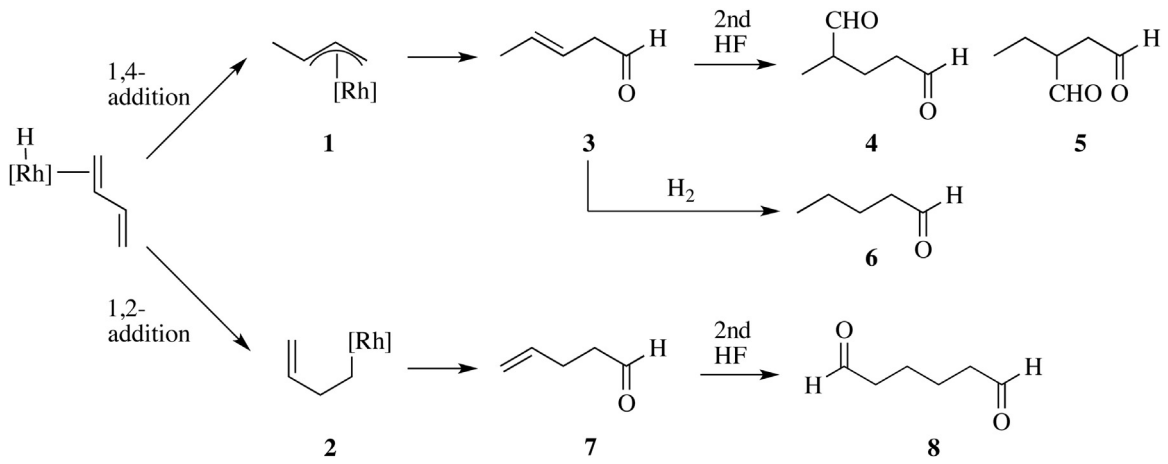


**Scheme 3.** (DIOP)Rh-catalyzed 1,3-butadiene hydroformylation products.

### 3.3. Isomerization-hydroformylation of Pent-3-enal (3)

To investigate the possibility that adipaldehyde arises from isomerization-hydroformylation, we started with freshly prepared toluene solutions of pent-3-enal (**3**) and subjected them to different hydroformylation conditions.

As depicted in Table 1, a significant amount of adipaldehyde, **8** was formed by hydroformylation of pent-3-enal (**3**) under various conditions. The effect of the syn-gas ($CO/H_2$ = 1:1) pressure was explored by varying it from 6 to 37 bar while keeping the temperature constant (Table 1, entries 1–4). These experiments demonstrate that the syn-gas pressure has only a minor influence on the selectivity for adipaldehyde. In contrast, varying the temperature (entries 5–7) decreases the aldipaldehyde selectivity compared to the reaction at 80 °C. In all cases pentanal (**6**) was the major byproduct that was observed. We note that it is difficult to quantitatively determine how much pentanal is produced at incomplete conversion, since both pent-3-enal and pentanal have similar retention times using our gas chromatographic method. However, $^1$H NMR spectra of the crude reaction mixture of entry 3 (after 3 h) showed the presence of pentanal (**6**) and adipaldehyde (**8**) in addition to starting pent-3-enal (**3**). Similar NMR spectroscopic analysis after 24 h showed complete consumption of **3** to adipaldehyde and pentanal. Importantly, the derivation of significant quantities of adipaldehyde from pent-3-enal shows that isomerizing hydroformylation is kinetically competent to occur during the hydroformylation of butadiene. Therefore, the formation of adipaldehyde (**8**) from hydroformylation of butadiene can be rationalized by a "normal" 1,2-addition pathway combined with a 1,4-addition hydroformylation-isomerization pathway involving the thermodynamically unfavorable isomerization of pent-3-enal (**3**) to pent-4-enal (**7**) followed by rapid linear selective hydroformylation to **8**.

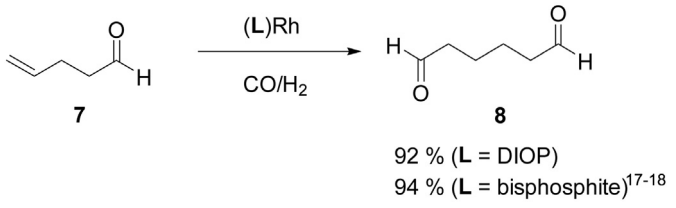


**Scheme 4.** Hydroformylation of pent-4-enal.

### 3.4. Computational results and discussion

In recent years density functional theory (DFT) calculations have been used to examine the reaction mechanisms of various transition-metal catalyzed isomerizations of alkenes yielding results in good agreement with experimental studies [30–32]. Thus, in order to better understand the experimental results presented above, we undertook a DFT study of the mechanism of isomerization of pent-3-enal (**3**) to pent-4-enal (**7**) and pent-2-enal. All DFT calculations reported in this work were carried out using the NWChem 6.5 quantum chemical software [33]. Structures were fully optimized using the M06-L functional [34] with the 6–31g* basis set on all atoms except Rh, for which the LANL2DZ effective core potential was used [35]. Harmonic frequency calculations were carried out to identify the stationary points as minima or transition states and to estimate the zero-point vibrational energy. To examine the isomerization of pent-3-enal to its isomers (Scheme 5) catalyzed by (DIOP)Rh, calculations were carried out for (a) hydride transfer from the (DIOP)Rh catalyst to pent-3-enal, and (b) β-hydride elimination of the resulting intermediates to produce the isomerization products, *i.e.,* the desired pent-4-enal and the undesired pent-2-enal.

In the (DIOP)Rh-catalyzed isomerization mechanism pathway (Scheme 5), pent-3-enal first coordinates to the Rh center *via* the alkene bond. Then, two possible isomerization pathways can occur from this reactant complex that differ in the destination of the hydride transferring from the catalyst to the bound pent-3-enal. In *path a* the hydride on the catalyst transfers to the C3 carbon of pent-3-enal resulting in the $\mathbf{Int}_a$ intermediate. Then β-hydride elimination from the C5 carbon chain of pent-3-enal will result in the desired pent-4-enal. Alternatively, $\mathbf{Int}_a$ can undergo β-hydride elimination from the C3 carbon to regenerate pent-3-enal, the reactant. In *path b* the hydride on the catalyst transfers to the C4 carbon of pent-3-enal to form the $\mathbf{Int}_b$ intermediate. Then β-hydride elimination from the C2 carbon of pent-3-enal will result in the undesired pent-2-enal, while β-hydride elimination from the C4 carbon will reform pent-3-enal, the reactant.

The calculated zero-point energy-corrected electronic energy profiles for the two pathways are shown in Fig. 1 and the corresponding structures of the stationary points are presented in Fig. 2. All reported electronic energies are relative to the reactant complex **R** (pent-3-enal coordinated to the (DIOP)Rh catalyst). We note that the reactant complex is a saturated 18 valence electron (VE) species with a trigonal bipyramidal structure. The minimum energy structure has the anionic hydride in the axial position and pent-3-enal is coordinated to the Rh center in the equatorial plane. The structure

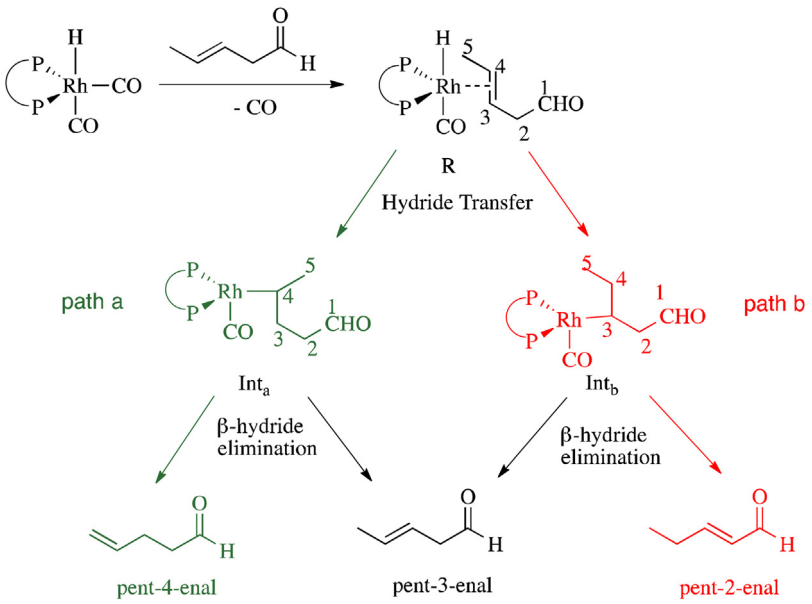


**Scheme 5.** (DIOP)Rh-catalyzed isomerization mechanism.

of the most stable conformer is shown in Fig. 2 (and the coordinates are given in the Supporting information).

The green curve ($\mathbf{R} \rightarrow \mathbf{TS}_{1a} \rightarrow \mathbf{Int}_a \rightarrow \mathbf{TS}_{2a} \rightarrow$ pent-4-enal) in Fig. 1 represents the energy profile for isomerization of pent-3-enal to the desired pent-4-enal. The first transition state, $\mathbf{TS}_{1a}$, corresponds to hydride transfer from Rh to the C3 carbon of pent-3-enal and has a barrier of $\Delta E^{\ddagger} = 11.7$ kcal/mol. This hydride transfer involves the rotation of the coordinated pent-3-enal out of the equatorial plane. In the $\mathbf{TS}_{1a}$ transition state structure (Fig. 2), the transferring hydride sits equidistant between the Rh and C3 carbon, with Rh—H and H—C3 distances of 1.67 Å. The resulting $\mathbf{Int}_a$ is a 16 VE complex with a distorted square planar geometry (shown in Fig. 2) and is stabilized relative to the bound pent-3-enal by 10.3 kcal/mol.

As noted above, two β-hydride elimination steps are possible from $\mathbf{Int}_a$. Elimination at the C3 carbon represents a return over the $\mathbf{TS}_{1a}$ barrier to the pent-3-enal reactant. While this route is unproductive, it is likely important in the reaction kinetics as it ties up both a (DIOP)Rh catalyst and a substrate molecule. Due to the lower energy of $\mathbf{Int}_a$, the barrier to reform pent-3-enal is 22.0 kcal/mol. If the hydride transfer instead occurs from the C5 carbon, the desired pent-4-enal is formed through the transition state $\mathbf{TS}_{2a}$. This bar-

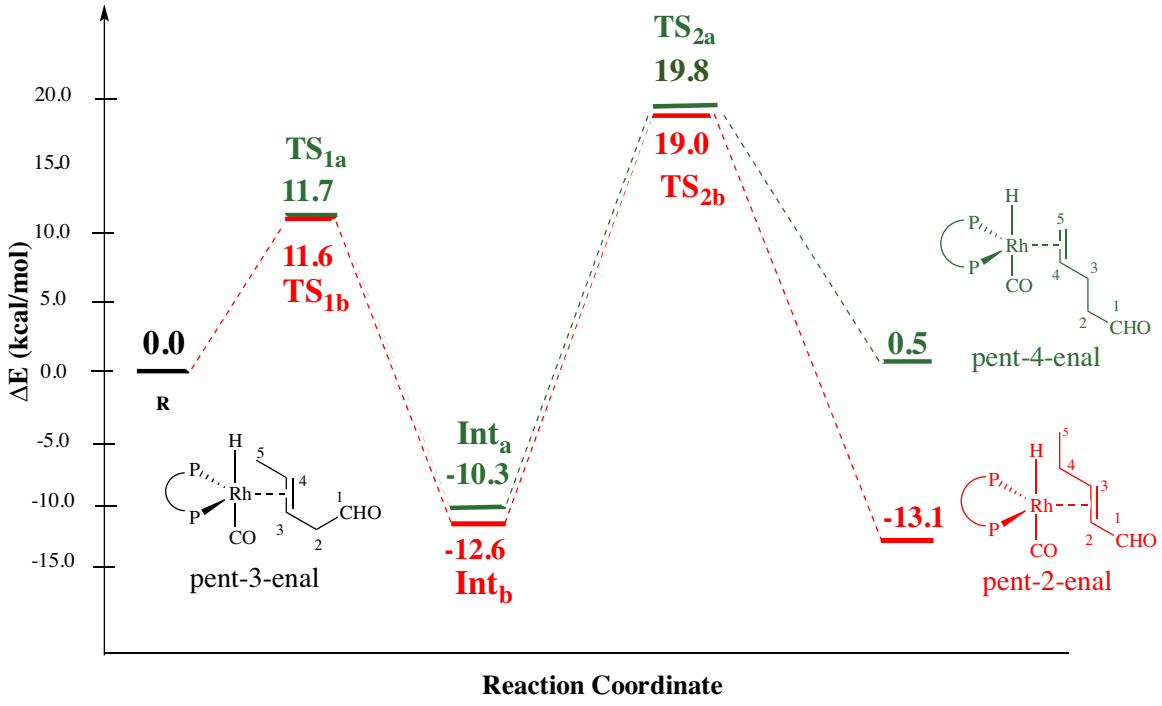


**Fig. 1.** Calculated zero point-corrected electronic energy profile for isomerization of pent-3-enal to pent-4-enal in green and isomerization of pent-3-enal to pent-2-enal in red. All energies are reported in kcal/mol with respect to the stable conformation of pent-3-enal coordinated to the Rh center (R). (For interpretation of the references to colour in this figure legend, the reader is referred to the web version of this article.)

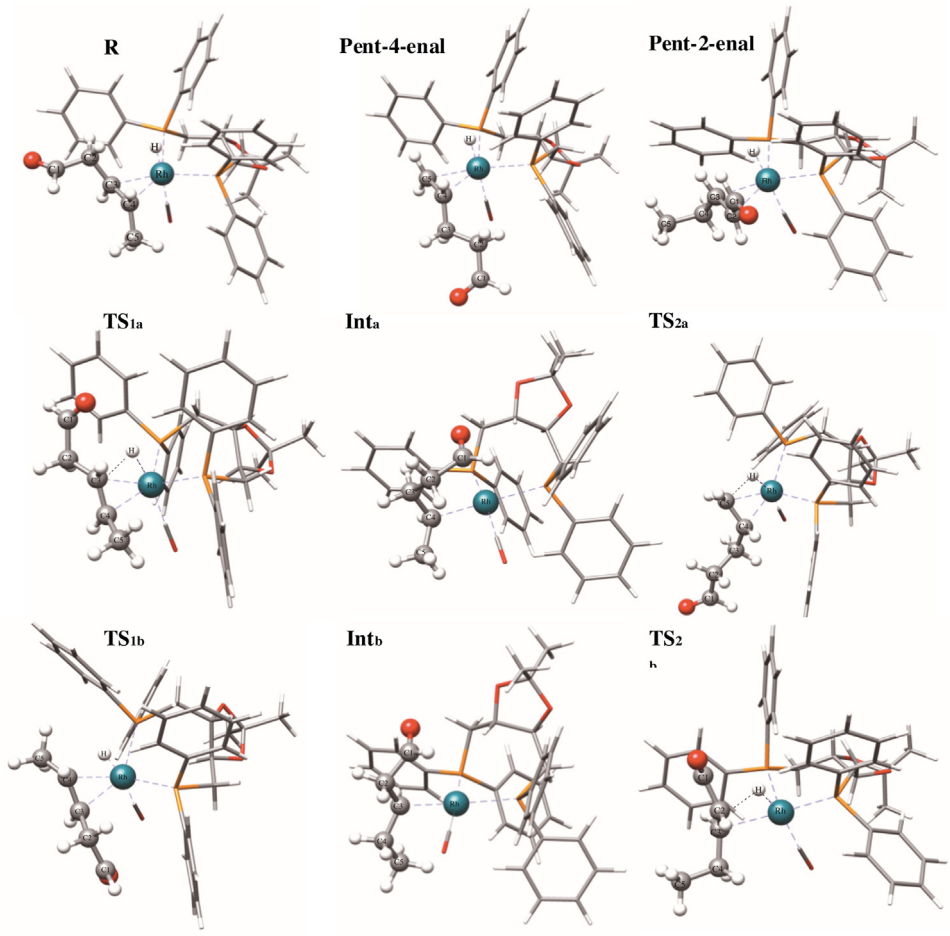


**Fig. 2.** Stationary point structures for *paths a* and *b* from the DFT calculations. First row: pent-3-enal (R), pent-4-enal, and pent-2-enal. Second row: $TS_{1a}$, $Int_a$, and $TS_{2a}$. Third row: $TS_{1b}$, $Int_b$, and $TS_{2b}$. Geometry parameters are shown in Table S1.

rier is higher than that to regenerate pent-3-enal, with a barrier of 30.1 kcal/mol relative to $\mathbf{Int}_a$. As with $\mathbf{TS}_{1a}$ the structure of $\mathbf{TS}_{2a}$ has the hydride directly between the Rh and C5 atoms with effectively the same Rh—H and H—C5 distances in both cases of 1.67 Å.

The red curve ($\mathbf{R} \rightarrow \mathbf{TS}_{1b} \rightarrow \mathbf{Int}_b \rightarrow \mathbf{TS}_{2b} \rightarrow$ pent-2-enal) in Fig. 1 represents the energy profile for isomerization of pent-3-enal to undesired pent-2-enal. As described above, $\mathbf{TS}_{1b}$, corresponds to hydride transfer from Rh to the C4 carbon of pent-3-enal, which requires the rotation of the coordinated pent-3-enal out of the equatorial plane, and has a barrier of $\Delta E^{\ddagger} = 11.6$ kcal/mol, In $\mathbf{TS}_{1b}$ (Fig. 2) the transferring hydride sits equidistant between Rh and the C4 carbon with Rh—H and H—C4 distances of 1.67 Å. Similar to the *path a* intermediate $\mathbf{Int}_a$, $\mathbf{Int}_b$ is also a 16 VE species with a distorted square planar geometry and is stabilized by 12.6 kcal/mol relative to **R**.

As described in Scheme 5, $\mathbf{Int}_b$ can also undergo two β-hydride elimination steps. Elimination at the C4 carbon leads to the formation of pent-3-enal (**R**) *via* $\mathbf{TS}_{1b}$ with a barrier of 24.2 kcal/mol, a step that is important in the overall reaction kinetics. If the hydride transfer occurs from the C2 carbon, the undesired isomer pent-2-enal is formed through the transition state $\mathbf{TS}_{2b}$ with a barrier of 31.6 kcal/mol. This barrier is higher than the barrier to form $\mathbf{Int}_b$ from **R**, and thus β-hydride elimination from the $\mathbf{Int}_b$ is the rate-limiting step. Further, as with all the other transition states ($\mathbf{TS}_{1a}$, $\mathbf{TS}_{2a}$, and $\mathbf{TS}_{1b}$), in the $\mathbf{TS}_{2b}$ structure the transferring hydride has identical Rh—H and H—C2 distances of 1.67 Å.

To model the solvent effects on the isomerization of pent-3-enal reaction, solvation model based on density (SMD) single-point calculations were carried out with toluene as the solvent. [36] The reaction energy profile is shown in Fig. S1 of the Supporting information. The results indicate that toluene solvent has only a minor effect on the reaction energetics. It does not change the relative ordering of the barriers with respect to formation of pent-4-enal and pent-2-enal. The key difference with respect to the gas phase results shown in Fig. 1 is that in the weakly polar toluene solvent the barriers are slightly larger, by ~1.2–4.6 kcal/mol. These small changes upon incorporating solvation indicate that gas phase calculations represent the relevant processes well.

It is interesting to compare the isomerization pathway of pent-3-enal to pent-4-enal (Fig. 1, green curve) with that for pent-3-enal isomerization to pent-2-enal (Fig. 1, red curve). The rate-limiting step in both cases is the second transition state ($\mathbf{TS}_{2a}$, and $\mathbf{TS}_{2b}$, respectively) from the intermediate to the pentenal product. The barriers for these two pathways are similar, 30.1 kcal/mol to form pent-4-enal compared to 31.6 kcal/mol to form pent-2-enal. However, both are larger than that for converting the respective intermediate back to pent-3-enal, 22 kcal/mol for $\mathbf{Int}_a$ and 24.2 kcal/mol for $\mathbf{Int}_b$. Thus, the calculations suggest that the rate-limiting barrier for pent-4-enal formation is less than that for pent-2-enal. However, the kinetics should be strongly influenced by the formation and decomposition of the intermediates $\mathbf{Int}_a$ and $\mathbf{Int}_b$, which involve substantially lower barriers.

The experimental results indicate that the isomerization of pent-3-enal in the presence of the (DIOP)Rh catalyst occurs to form both pent-4-enal and pent-2-enal, with the latter the major product. An additional consideration in examining these results is that

pent-2-enal is the most stable isomer and is thus the thermodynamically favored isomer. This is enhanced upon binding to the (DIOP)Rh catalyst, which further stabilizes the pent-2-enal isomer compared to the (DIOP)Rh-bound pent-3-enal and pent-4-enal forms. Moreover, pent-2-enal bound to the (DIOP)Rh catalyst is stabilized by 13.1 and 13.6 kcal/mol relative to the catalyst-bound pent-3-enal and pent-4-enal, respectively (Fig. 1). These relative stabilities are modified compared to the isolated pentenals, where pent-2-enal is 5.0 and 9.3 kcal/mol more stable than pent-3-enal and pent-4-enal, respectively. The (DIOP)Rh-bound pent-2-enal appears to be further favored over the other two isomers due to favorable interactions of the aldehyde group with a ligand phenyl ring.

After isomerization, pent-4-enal can undergo a hydroformylation to form adipaldehyde; this is expected to be rapid but must compete with reformation of **Int**$_a$ *via* **TS**$_{2a}$ as shown in Fig. 1. In contrast, the hydroformylation of pent-2-enal is expected to be slower. Fig. 1 also indicates that return to the intermediate (**Int**$_b$ *via* **TS**$_{2b}$) should be less likely for pent-2-enal due to the substantially larger barrier of 32.1 kcal/mol (compared to the same process for pent-4-enal). On the other hand, pent-2-enal can also undergo a hydrogenation reaction to form pentanal side product.

## 4. Conclusions

Isomerization of pent-3-enal to pent-4-enal, leading to adipaldehyde formation through subsequent hydroformylation, has been demonstrated using the (DIOP)Rh catalyst. The thermodynamically favored isomer, pent-2-enal, is also formed and represents the major isomerization product; pent-2-enal is identified through the products of its subsequent and hydrogenation. While the yield of pent-4-enal is low, the results support the notion that its hydroformylation is rapid and thus an isomerization catalyst may be used to direct the branching of butadiene hydroformylation toward adipaldehyde formation.

A DFT study of the reaction pathways has been carried out to better understand the experimental results. The energy profiles for pent-3-enal isomerization to both pent-2-enal and pent-4-enal have been determined. They indicate that the barriers to form the two isomers are similar. The lowest barriers are for forming intermediates, that can then lead to pent-2-enal or pent-4-enal, by hydride transfer from the catalyst to pent-3-enal and its reverse reaction. Thus, the overall reaction kinetics are expected to depend not only on the barriers to isomerization alone, but the equilibria between (DIOP)Rh-bound pent-3-enal and these intermediates.

## Acknowledgement

We thank the NSF-EPA Networks for Sustainable Materials Design and Synthesis (NSMDS) under NSF Grant CHE-1339661 for funding.

## Appendix A. Supplementary data

Supplementary data associated with this article can be found, in the online version, at http://dx.doi.org/10.1016/j.molcata.2016.08.021.

## References

[1] H.-J. Arpe, Industrielle Organische Chemie, Bedeutende Vor- und Zwischenprodukte, Wiley-VCH Weinheim, 2007, pp. 138.
[2] H.-J. Arpe, K. Weissermel, Industrial Organic Chemistry, Wiley-VCH Weinheim, 2010.
[3] K. Weissermel, H.-J. Arpe, Industrial Organic Chemistry, 4th ed., Wiley-VCH Weinheim, Germany, 2003.
[4] G. Bellussi, C. Perego, Industrial catalytic aspects of the synthesis of monomers for nylon production, Cattech 4 (2000) 4–16.
[5] R. Franke, D. Selent, A. Börner, Applied hydroformylation, Chem. Rev. 112 (2012) 5675–5732.
[6] S. Van de Vyver, Y. Román-Leshkov, Emerging catalytic processes for the production of adipic acid, Catal. Sci. Technol. 3 (2013) 1465–1479.
[7] Teles, B. Roessler, R. Pinkos, T. Genger, T. Preiss, Method for Producing Cyclododecanone. WO2005030689A2, May 26, (2005).
[8] B.D. Herzog, R.A. Smiley, Ullmann's Encyclopedia of Industrial Chemistry, Wiley-VCH Weinheim, Germany, 2000.
[9] P.W.N.M. Van Leeuwen, J. Frauendiener, R. Penrose Kluwer, Homogenous Catalysis Understanding the Art, Academic Publishers, Dordrecht, 2004, pp. 231.
[10] M.E. Tauchert, D.C. Warth, S.M. Braun, I. Gruber, A. Ziesak, F. Rominger, P. Hofmann, Highly efficient nickel-catalyzed 2-methyl-3-butenenitrile isomerization: applications and mechanistic studies employing the TTP ligand family, Organometallics 30 (2011) 2790–2809.
[11] P. Hofmann, M.E. Tauchert, Molecular Catalysis, Wiley-VCH Weinheim, Germany, 2014, pp. 161.
[12] A.P. Göthlich, M. Tensfeldt, H. Rothfuss, M.E. Tauchert, D. Haap, F. Rominger, P. Hofmann, Novel chelating phosphonite ligands: syntheses, structures, and nickel-catalyzed hydrocyanation of olefins, Organometallics 27 (2008) 2189–2200.
[13] K.-S. Chen, T.L. Yu, Y.-S. Chen, T.-L. Lin, W.-J. Liu, Soft-and hard-segment phase segregation of polyester-based polyurethane, J. Polym. Res. 8 (2001) 99–109.
[14] G. Teng, F.N. Jones, End-grafting of oligoesters based on terephthalic acid and linear diols for high solids coatings, J. Appl Polym. Sci. 60 (1996) 1609–1618.
[15] T. Kiyotsukuri, N. Takemoto, N. Tsutsumi, W. Sakai, M. Nagata, Regular network polyesters from benzenepolycarboxylic acids and glycol, Polymer 36 (1995) 5045–5049.
[16] Y. Ohgomori, N. Suzuki, N. Sumitani, Formation of 1 6-hexanedial via hydroformylation of 1, 3-butadiene, J. Mol. Catal. A: Chem. 133 (1998) 289–291.
[17] S.E. Smith, T. Rosendahl, P. Hofmann, Toward the rhodium-catalyzed bis-hydroformylation of 1, 3-Butadiene to adipic aldehyde, Organometallics 30 (2011) 3643–3651.
[18] J. Mormul, M. Mulzer, T. Rosendahl, F. Rominger, M. Limbach, P. Hofmann, Synthesis of adipic aldehyde by n-selective hydroformylation of 4-pentenal, Organometallics 34 (2015) 4102–4108.
[19] J. Briggs, D. Packett, D. Bryant, A. Phillips, D. Schreck, K. Olson, E. Tjaden, A. Guram, T. Eisenschmid, E. Bragham, Process for Producing Hydroxyaldehydes, WO199740001A1 Oct. 30, (1997).
[20] C. Botteghi, M. Branca, A. Saba, Optically active aldehydes via hydroformylation of 1, 3-dienes with chiral diphosphinerhodium complexes, J. Organomet. Chem. 184 (1980) C17–C19.
[21] B. Fell, P. Hermanns, H. Bahrmann, J. Prakt. Chem. Ztg. 340 (1998) 459–467.
[22] H. Bahrmann, B. Fell, The hydroformylation of conjugated dienes VI tertiary aryl-and arylalkyl-phosphines and secondary alkyl-and arylphosphines as ligands in the rhodium catalyzed hydroformylation reaction of conjugated dienes to dialdehydes, J. Mol. Catal. 8 (1980) 329–337.
[23] D.L. Packett, Hydroformylation Process for Producing 1,6-Hexandials, U.S. Patent 5,312,996, May 17, (1994).
[24] J. Mormul, J. Breitenfeld, O. Trapp, R. Paciello, T. Schaub, P. Hofmann, Synthesis of adipic acid, 1, 6-hexanediamine, and 1 6-hexanediol via double-n-selective hydroformylation of 1, 3-butadiene, ACS Catal. 6 (2016) 2802–2810.
[25] J. Ternel, J.L. Couturier, J.L. Dubois, J.F. Carpentier, Rhodium-catalyzed tandem isomerization/hydroformylation of the bio-sourced 10-undecenenitrile: selective and productive catalysts for production of polyamide-12 precursor, Adv. Synth. Catal. 355 (2013) 3191–3204.
[26] A. Behr, D. Obst, A. Westfechtel, Isomerizing hydroformylation of fatty acid esters: formation of ω-aldehydes, Eur. J. Lipid Sci Technol. 107 (2005) 213–219.
[27] Y. Yuki, K. Takahashi, Y. Tanaka, K. Nozaki, Tandem isomerization/hydroformylation/hydrogenation of internal alkenes to n-alcohols using Rh/Ru dual-or ternary-catalyst systems, J. Am. Chem. Soc. 135 (2013) 17393–17400.
[28] C.J. Scheuermann née, C. Taylor, Jaekel, Enantioselective hydrogenation of enones with a hydroformylation catalyst, Adv. Synth. Catal. 350 (2008) 2708–2714.
[29] T. Ohshima, H. Tadaoka, K. Hori, N. Sayo, K. Mashima, Highly enantio-and S-trans CC bond selective catalytic hydrogenation of cyclic enones: alternative synthesis of (−)-Menthol, Chem. Eur. J. 14 (2008) 2060–2066.
[30] M.A.n. Carvajal, S. Kozuch, S. Shaik, Factors controlling the selective hydroformylation of internal alkenes to linear aldehydes 1. The isomerization step, Organometallics 28 (2009) 3656–3665.
[31] J. Tao, F. Sun, T. Fang, Mechanism of alkene isomerization by bifunctional ruthenium catalyst: a theoretical study, J. Organomet. Chem. 698 (2012) 1–6.
[32] S. Biswas, Z. Huang, Y. Choliy, D.Y. Wang, M. Brookhart, K. Krogh-Jespersen, A.S. Goldman, Olefin isomerization by iridium pincer catalysts. experimental evidence for an η3-Allyl pathway and an unconventional mechanism predicted by DFT calculations, J. Am. Chem. Soc. 134 (2012) 13276–13295.
[33] M. Valiev, E.J. Bylaska, N. Govind, K. Kowalski, T.P. Straatsma, H.J. Van Dam, D. Wang, J. Nieplocha, E. Apra, T.L. Windus, N.W. Chem, A comprehensive and scalable open-source solution for large scale molecular simulations, Comp. Phys. Comm. 181 (2010) 1477–1489.

[34] Y. Zhao, D.G. Truhlar, The M06 suite of density functionals for main group thermochemistry, thermochemical kinetics, noncovalent interactions, excited states, and transition elements: two new functionals and systematic testing of four M06-class functionals and 12 other functionals, Theor. Chem. Acc. 120 (2008) 215–241.
[35] M. Kumar, R.V. Chaudhari, B. Subramaniam, T.A. Jackson, Ligand effects on the regioselectivity of rhodium-catalyzed hydroformylation: density functional calculations illuminate the role of long-range noncovalent interactions, Organometallics 33 (2014) 4183–4191.
[36] A.V. Marenich, C.J. Cramer, D.G. Truhlar, Universal solvation model based on solute electron density and on a continuum model of the solvent defined by the bulk dielectric constant and atomic surface tensions, J. Phys. Chem. B 113 (2009) 6378–6396.